Article

Discovery Medicine 2024; 36(186): 1430–1440
https://doi.org/10.24976/Discov.Med.202436186.133

SIRT6 Inhibits the Proliferation and Collagen Synthesis of Keloid Fibroblasts through MAPK/ERK Pathway

Tao Zhou[1,*], Yajie Chen[2], Chao Wang[1], Zhiyong Huang[1], Ziming Tan[1], Yan Ma[1]

[1]Department of Burn and Plastic Surgery, Chengdu Second People's Hospital, 610021 Chengdu, Sichuan, China
[2]State Key Laboratory of Trauma, Burn and Combined Injury, Institute of Burn Research, Southwest Hospital, Third Military Medical University (Army Medical University), 400038 Chongqing, China
*Correspondence: zhoutaoly@163.com (Tao Zhou)
Published: 20 July 2024

Background: Keloid, a fibroproliferative disorder, significantly impacts patients' quality of life, yet effective therapies remain elusive. This study explored the role of silent information regulator 6 (SIRT6) in modulating the proliferation, invasion, and collagen synthesis of keloid fibroblasts.

Methods: Keloid and normal skin specimens were collected, and fibroblasts were isolated from the keloid tissue. SIRT6 recombinant adenovirus (Ad) was constructed to infect keloid fibroblasts to overexpress SIRT6. This study entails three groups: Control group, adenovirus-Negative Control (Ad-NC) group, and Ad-SIRT6 group. SIRT6 protein and mRNA levels were measured via Western blotting and Quantitative reverse transcription polymerase chain reaction (qRT-PCR), respectively. Cell viability was determined using 5-ethynyl-2′-deoxyuridine (EdU) assay. Flow cytometry was exploited to measure cell apoptosis. To investigate cell migration, wound healing assay and Transwell assay were employed. Western blotting was also utilized to study the expression levels of apoptotic proteins, collagen deposition-related proteins, and Mitogen-Activated Protein Kinases (MAPK)/extracellular regulated protein kinases (ERK) pathway-related proteins.

Results: Compared to the control and Ad-NC groups, the Ad-SIRT6 group exhibited significantly elevated SIRT6 level; diminished cell proliferation, migration and invasion; reduced protein levels of α-smooth muscle actin (α-SMA), collagen I, collagen III, phospho SMAD Family Member 3 (p-Smad3), transforming growth factor-β 1 (TGF-β1), and MAPK/ERK pathway proteins (phospho extracellular signal-regulated protein kinase 1/2 (p-ERK1/2), phospho MAP kinase-ERK kinase (p-MEK) and phospho-c-Raf (p-c-Raf)). Treatment with epidermal growth factor (EGF), an MAPK/ERK pathway agonists, reversed the inhibitory effect of SIRT6 on cell activity and inhibited apoptosis in keloid fibroblasts.

Conclusion: SIRT6 overexpression in keloid fibroblasts attenuates proliferation, invasion, and collagen synthesis, while fostering apoptosis, likely through the suppression of MAPK/ERK pathway activity. This suggests a potential therapeutic target for keloid treatment.

Keywords: keloid; fibroblasts; SIRT6; collagen synthesis; MAPK/ERK signaling pathway

Introduction

Keloid is a common benign proliferative disease of the skin, which is often accompanied by pain, itching, allergy and other symptoms, and is at risk of causing ulceration, infection, spoiled appearance, and severe negative impacts on the physical and mental health of patients [1]. At present, although many methods for treating keloid are available, none of the commonly used treatment methods, including topical medicines, compression therapy, laser, surgery and radiation therapy, produce satisfactory curative effects, and yet comprehensive treatment remains the first treatment option in clinical settings [2,3]. Therefore, treating keloids is still a major challenge in the realm of plastic surgery. Abnormal proliferation of fibroblasts and excessive deposition of collagen are closely related to the pathogenesis of keloid [4]. At present, the molecular mechanisms underlying keloid formation and growth, involving fibroblasts remains unclear [5]. Thus, it is imperative to identify genes with key regulatory effects on collagen synthesis of keloid fibroblasts because it can deepen the comprehension of the keloid fibroblasts for the general public and explore new therapeutic targets for keloid treatment.

As a member of the sirtuins family of histone deacetylases, silent information regulator 6 (SIRT6) is involved in modulating biological functions and participating in the pathogenesis of metabolic diseases, cardiovascular and cerebrovascular diseases, tumors and other diseases [6]. SIRT6 has been discovered to have a huge involvement in the process of fibrosis, and its mechanism is closely associated with the modulation of Mitogen-Activated Protein Kinases (MAPK)/extracellular regulated protein kinases (ERK) signaling pathway [7]. SIRT6 plays a crucial role in modulating the biological functions of fibrob-

lasts and inhibits the differentiation of fibroblasts into myofibroblasts, thereby delaying the onset and progression of aging-related organ fibrosis [8]. In adventitial fibroblasts, SIRT6 inhibits angiotensin II induced cell proliferation, migration, and collagen production [9]. Additionally, SIRT6 can inhibit the proliferation and collagen synthesis of dural scar fibroblasts and play an important role in the formation of dural scar caused by laminectomy [10]. Nevertheless, whether SIRT6 is involved in the modulation of fibrotic process of keloid has not been investigated. In this study, we aimed to study the role of SIRT6 in regulating the proliferation and collagen synthesis of keloid fibroblasts, as well as the molecular mechanisms involved. Overexpression of SIRT6 in keloid fibroblasts by means of adenovirus-mediated gene overexpression could effectively inhibit cell proliferation and collagen synthesis, suggesting that SIRT6 has an inhibitory function for abnormal activation of keloid fibroblasts. Therefore, targeting SIRT6 to develop new therapeutic methods for keloid stands out as a promising avenue.

Materials and Methods

Fibroblast Isolation and Culture

Fibroblasts were extracted from keloid tissue specimens and cultured *in vitro*. Keloid and normal skin specimens were acquired from patients who underwent keloid resection in Chengdu Second People's Hospital. This study adheres to the ethical principles of the Helsinki Declaration and was approved by the Chengdu Second People's Hospital ethics committee (No. 2023927723). The selected patients did not receive any treatment to suppress scar hyperplasia, and did not suffer any systemic effect. These patients provided their medical history, as well as informed consent to join this research.

The subcutaneous tissue was removed from the obtained specimens, and the tissue was cut into 2 mm $\times$ 2 mm. The trimmed tissue pieces were then placed at the center of each well in a 6-well plate. The specimens were covered with a 22 mm cover glass slide while they were incubated in a CO_2 incubator set at 37 °C for 6–8 h. When the cells became firmly adhered to the wall in the culture dish, Dulbecco's Modified Eagle Medium (DMEM, 11995065, Thermo Scientific, Waltham, MA, USA) was added to ensure continued cell cultivation. The cells were observed every day and the culture medium was changed once every 3 days. When the cells had grown into a monolayer, 0.25% trypsin was added for digestion. Cells that have fully grown were passaged in a 1:3 ratio. Cells were then cultivated in culture medium, which was replaced once every 2 to 3 days. Cells were passaged once in 4 to 5 days until the third passage, and the cells were observed under the microscope (ECLIPSE Ts2, Nikon, Tokyo, Japan).

Fibroblasts in good proliferative state were passaged, and 1 $\times$ 10^6 cells were collected in 1 mL Eppendorf tubes. The cell suspensions were centrifuged at 1000 rpm for 5 min, with a centrifugation radius of 10 cm. Phosphate-buffered saline (PBS) was discarded, and the cells were pre-fixed with 2.5% glutaraldehyde, post-fixed with 1% osmium, and dehydrated stepwise in ethanol. After embedding sections in resin, they were double-stained with uranyl acetate (Yunxing Biology, RG-A260338, Shaoguan, China) and lead citrate (Beyotime, 512-265, Shanghai, China), and then observed under a transmission electron microscope (JEM-2000EX, JEOL company, Tokyo, Japan).

Adenovirus Infections and Grouping

The origin of the primary cells was confirmed using the approved DNA-based method. The identity of the cells was confirmed by checking against a cell line database established by ICLAC. Short tandem repeat (STR) analysis was performed, and cross-contamination and Mycoplasma contamination were not detected.

In 96-well plates, keloid fibroblasts were inoculated (3 $\times$ 10^3 cells/well). Adenoviruses were added at a multiplicity of infection (MOI) of 50. The infection efficiency was enhanced by adding 4 µg/mL polybrene. After being refreshed with the new medium, the cells were returned to the incubator for an additional incubation for 48 h. Keloid fibroblasts were separated into three groups: control group, adenovirus-Negative Control (Ad-NC) group, and Ad-SIRT6 group. For the control group, the cells were not subjected to any treatment; the cells in the Ad-NC group were infected with control adenovirus; the cells in the Ad-SIRT6 group were infected with SIRT6 overexpression adenovirus. After adenovirus infections, the cells were cultured further for 72 h prior to subsequent experimental assays. Cells were treated with MAPK/ERK pathway agonists epidermal growth factor (EGF) to validate the role of the MAPK/ERK pathway. After transfection with Ad-SIRT6, keloid fibroblasts was treated with 10 ng/mL EGF (AF-100-15-1MG, Thermo Fisher Scientific, Waltham, MA, USA) for 24 h.

Quantitative Reverse Transcription Polymerase Chain Reaction (qRT-PCR)

Total RNA was extracted from the cultured cells using Trizol reagent (Thermo Fisher Scientific, 15596018CN, Waltham, MA, USA). A 20 µL reaction was formed by including 1 µg total RNA, reverse transcriptase solution, buffer, and reverse transcription primers, reconstituted with RNase-free water. The reverse transcription reaction conditions were set as follows: 37 °C, 15 min; 85 °C, 5 s. A 25 µL reaction for qRT-PCR was formed by including 2 µL reverse transcription reaction products, TB Green Fast qPCR Mix (A15297, Baobioengineering Co., Ltd., Dalian, China), and forward and reverse primers, topped up with sterile water. qRT-PCR reaction conditions were set as follows: 95 °C, 30 min; 95 °C, 5 s; and 60 °C, 10 s (40 cycles). Utilizing the $2^{-\Delta\Delta Ct}$, the relative mRNA levels of *SIRT6*

were calculated, with glyceraldehyde 3-phosphate dehydrogenase (*GAPDH*) being used as the internal reference gene. The primer sequences are given below:

SIRT6 forward primer: 5′-CCCGGATCAACGGCTC TATC-3′

SIRT6 reverse primer: 5′-GCCTTCACCCTTTTGG GGG-3′

GAPDH forward primer: 5′-GTCTCCTCTGACTTC AACAGCG-3′

GAPDH reverse primer: 5′-ACCACCCTGTTGCTG TAGCCAA-3′

Western Blotting

Proteins from cells were extracted using a protein extraction kit. Protein concentration was determined via the BCA protein quantification kit (P0012, Beyotime, Shanghai, China). Protein samples (30 µg) was added to each well of the gel for SDS-PAGE electrophoresis. The separated proteins on the gel were then the PVDF membrane. The PVDF membrane was blocked for 1 h at room temperature. Diluted solutions for primary antibodies were prepared: SIRT6 (1:1000, ab88494), Bcl-2-associated X protein (Bax) (1:1000, ab32503), B-cell lymphoma-2 (Bcl-2) (1:1000, ab182858), α-smooth muscle actin (α-SMA) (1:1000, ab240678), collagen I (1:1000, ab138492), collagen III (1:1000, ab184993), phospho SMAD Family Member 3 (p-Smad3, 1:1000, ab52903), Smad3 (1:1000, ab40854), transforming growth factor-β 1 (TGF-β1, 1:1000, ab142139), phospho extracellular signal-regulated protein kinase 1/2 (p-ERK1/2, 1:1000, ab126445), phospho MAP kinase-ERK kinase (p-MEK, 1:1000, ab307509), phospho-c-Raf (p-c-Raf, 1:1000, ab120428), ERK1/2 (1:1000, ab17942), MEK (1:1000, ab32576), c-Raf (1:1000, ab137435), and GAPDH (1:2000, ab8245). These antibodies were obtained from abcam (Shanghai, China). The PVDF membrane was incubated in diluted primary antibody solution at 4 °C overnight. After the incubation, the membrane was washed with TBS with Tween (TBST, Thermo Fisher Scientific, BL315B, Waltham, MA, USA) and then incubated with Horseradish peroxidase (HRP)-labeled sheep anti-rabbit secondary antibody (1:2500, Proteintech Group, Inc, Wuhan, China) for 1 h at room temperature. Afterward, the membrane was washed with TBST, and the enhanced chemiluminescence (ECL) reagent (Thermo Fisher Scientific, 32209, Waltham, MA, USA) was uniformly applied to the membrane, which was then placed in a gel imager for exposure and image acquisition. Image J (Image J 21, NIH, Bethesda, MA, USA) was used to analyze the gray value of each protein.

EdU Assay

In 6-well culture plates (containing coverslips), keloid fibroblasts were inoculated. For achieving a final concentration of 10 µmol/L, an equal volume of 5-ethynyl-2′-deoxyuridine (EdU) working solution was supplemented. The cells were continued to be incubated for 2 h in an incubator. The culture medium was subsequently removed, and 4% paraformaldehyde was supplemented for fixation for 15 min at room temperature. After removing the fixative, the cells were washed with PBS and incubated with PBS (including 0.3% Triton X-100) for 15 min. After the removal of the permeabilizing solution, cells were washed with PBS and added to EdU reaction solution. For ensuring that the reaction mixture can cover the sample evenly, the plate was shaken gently. The plate was incubated for 30 min at room temperature away from light. 4′,6-diamidino-2-phenylindole (DAPI) solution was added for re-staining after removing the reaction solution, and incubated for 10 min at room temperature away from light. Washing with PBS and film sealing using an anti-fluorescence quenching sealing solution were performed, followed by observation and image acquisition under a fluorescence microscope (EVOS™ M7000, Thermo Fisher Scientific, AMF7000, Waltham, MA, USA).

Flow Cytometry

In 6-well plates, 4×10^5 cells per well were inoculated and cultured in DMEM medium supplemented with 10% fetal bovine serum for 48 h. Trypsin digestion was subsequently performed, and the cell suspension was centrifuged. The cells of each group were collected in 1.5 mL Eppendorf tubes. Binding buffer (500 µL) was added to each tube for suspending the cells. Annexin V-FITC (5 µL) and PI (10 µL) were added to the cell suspensions and mixed well. The cell mixtures were left to stand at room temperature away from light for about 20 min. Cell apoptosis was then measured by means of flow cytometry (BD FACSAria™ Fusion, Thermo Fisher Scientific, Waltham, MA, USA).

Wound Healing Assay

The density of cells remaining at logarithmic growth phase was adjusted to 5×10^5 cells per well. The cell suspension was inoculated to a 6-well plate (2 mL per well), with the purpose of cultivating a monolayer of cells in each well. The cells were incubated in a cell culture incubator for 24 h. A straight line was streaked on the cell monolayer at bottom of the plate using a sterile 200 µL tip. With sterile PBS solution, the exfoliated cells were washed, photographed with an inverted microscope at 0 and 24 h, respectively. The rate of cell migration was calculated using the formula given below:

Cell migration rate (%) = (Scratch width at 0 h – Scratch width at a time point)/Scratch width at 0 h $\times$ 100

Transwell Assay

Keloid fibroblasts were collected and resuspended in serum growth factor-free medium and adjusted to a cell density of 5×10^4 cells/mL. Cell suspension (200 µL) was added to the upper chamber of the Transwell lined with matrix gel. Medium (500 µL) supplemented with 20% FBS

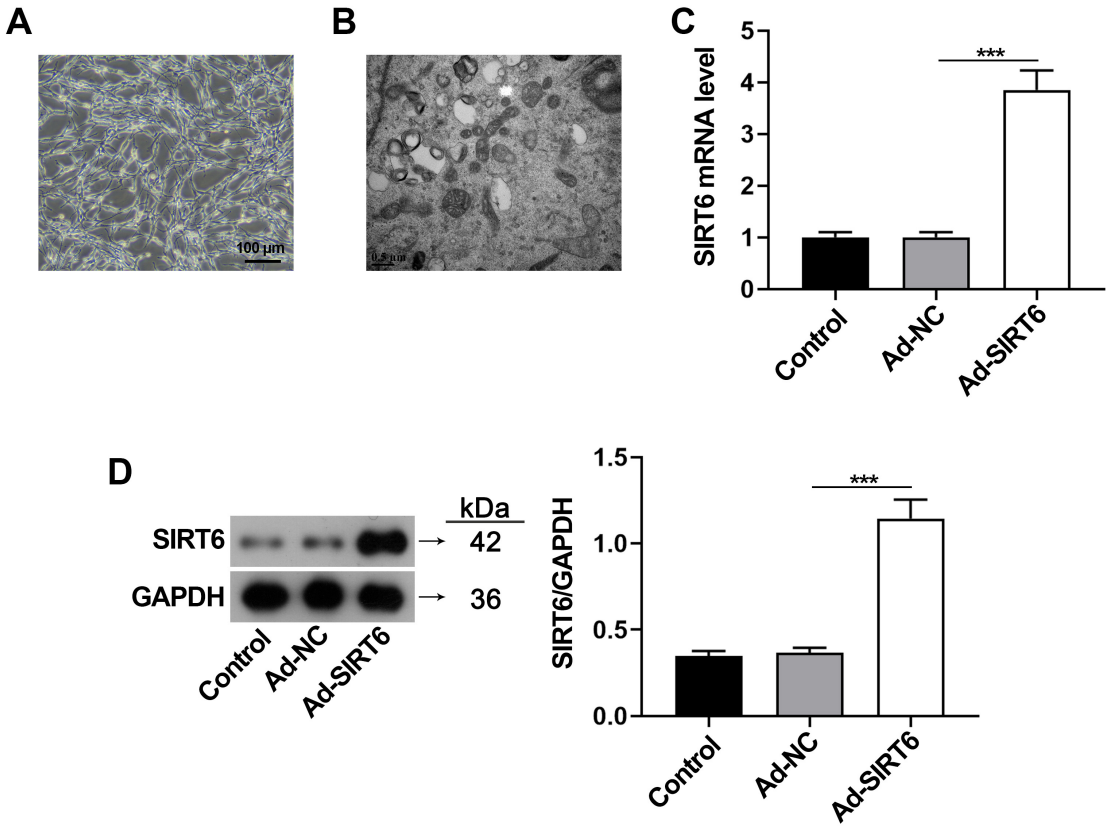

Fig. 1. Effect of Ad-SIRT6 infection on STRT6 levels in keloid fibroblasts. (A) Morphology of fibroblasts under an inverted microscope. (B) Identification of keloid fibroblast ultrastructure by means of transmission electron microscopy. (C) *SIRT6* mRNA level following the Ad-SIRT6 infection. (D) SIRT6 protein level following the Ad-SIRT6 infection. ***$p < 0.001$, versus Ad-NC subgroup. n = 3. Ad, adenovirus; SIRT6, silent information regulator 6; GAPDH, glyceraldehyde 3-phosphate dehydrogenase; Ad-NC, adenovirus-Negative Control.

was added to the lower chamber. The Transwell device was placed into the cell culture incubator. After 24 h, the small chamber was removed, the excess liquid was aspirated from the upper chamber, which was gently rotated with a cotton swab to wipe off the residual cells. 4% paraformaldehyde solution was added for fixation for 30 min. After washing with PBS and staining with crystal violet solution for 10 min, the staining solution was slowly washed away with running water. After air-drying, microscope (ECLIPSE Ts2, Nikon, Tokyo, Japan) observation and image acquisition were performed.

Statistical Analysis

Experimental data were processed and analyzed using GraphPad Prism 8 (GraphPad Software, San Diego, CA, USA). Experimental data are expressed as mean ± standard deviation. The experimental data of any two groups were statistically analyzed using independent samples *t*-test, whereas the experimental data of three and more groups were statistically analyzed using one-way analysis of variance (ANOVA), coupled with post-hoc Tukey test. Differences were considered statistically significant at $p < 0.05$.

Results

Effect of Infection with Ad-SIRT6 on STRT6 Levels in Keloid Fibroblasts

Tissue blocks were cultured for 7 days with fibroblast sprouting, showing filamentous phenotype. After 14 days, fibroblasts sprouted from most of the tissue mass, manifesting accelerated cell growth, and the tissue mass left the wall successively. After 21 days, 90% of the primary cells were fused, the cells formed irregular arrangements, and the individual cells became irregularly pike-shaped with full cytoplasm (Fig. 1A).

Fibroblasts attained accelerated growth, forming monolayer within 3 days of incubation, showing a cluster distribution and a tight but irregular arrangement. The cells were spindle-shaped and irregularly shaped, with a full cytoplasm and 1–2 oval-shaped nucleoli (Fig. 1B). SIRT6 expression was substantially elevated in the Ad-SIRT6 group compared to the control and Ad-NC groups, which was confirmed with qRT-PCR and Western blotting (Fig. 1C,D, $p < 0.001$).

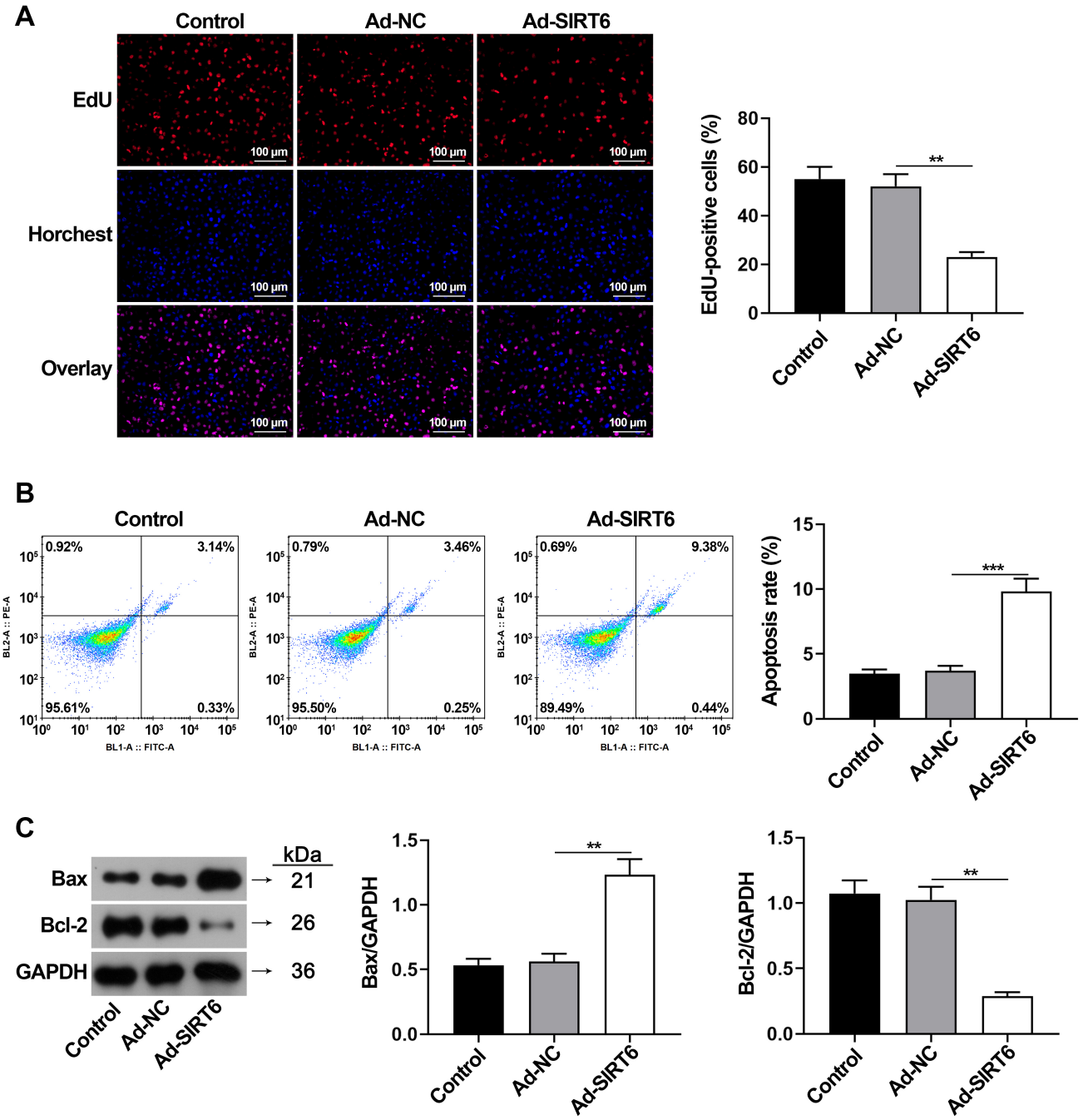

Fig. 2. Effect of SIRT6 overexpression on proliferation and apoptosis of keloid fibroblasts. (A) Cellular activity of keloid fibroblasts visualized by EdU assay. (B) Flow cytometry analysis of cell apoptosis. (C) Determination of Bax and Bcl-2 protein levels. $^{**}p < 0.01$, $^{***}p < 0.001$, versus Ad-NC subgroup. n = 3. EdU, 5-ethynyl-2′-deoxyuridine; Bax, Bcl-2-associated X protein; Bcl-2, B-cell lymphoma-2.

Effect of SIRT6 Overexpression on Proliferation and Apoptosis of Keloid Fibroblasts

Subsequently, we assessed the effects of Ad-SIRT6 infection on keloid fibroblast activity and apoptosis. In the Ad-SIRT6 group, EdU-positive cell rate was significantly lower than in the control and Ad-NC groups (Fig. 2A, $p < 0.01$). Flow cytometry analysis revealed that cell apoptosis was substantially augmented in the Ad-SIRT6 group as compared to the control and Ad-NC groups (Fig. 2B, $p < 0.001$). Western blotting results showed that Bax protein level was substantially increased while Bcl-2 protein level was significantly reduced in the Ad-SIRT6 group compared to the control and Ad-NC groups (Fig. 2C, $p < 0.01$), suggesting that Ad-SIRT6 infection inhibits keloid fibroblast proliferation and promotes apoptosis.

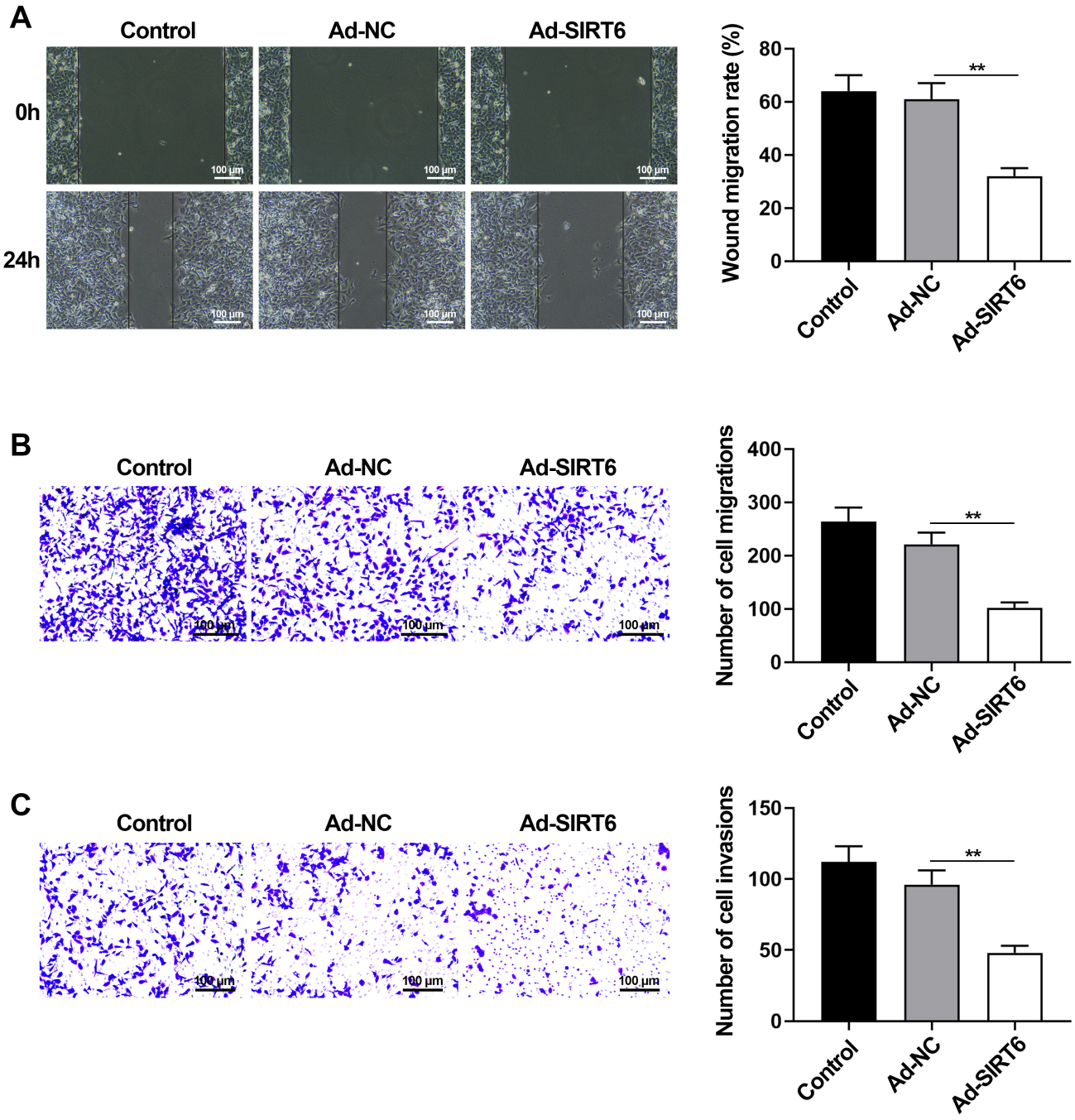

Fig. 3. Effect of SIRT6 overexpression on keloid fibroblast migration. (A) Analysis of cell migration in wound healing assay. (B,C) Determination of cell migration and invasion in Transwell assay. $^{**}p < 0.01$. n = 3.

Effect of SIRT6 Overexpression on Migration of Keloid Fibroblasts

The wound migration distance was significantly shorter in the Ad-SIRT6 group than in the control and Ad-NC groups, as revealed by the wound healing assay (Fig. 3A, $p < 0.01$). The migrating and invading cells in the Ad-SIRT6 group were less than those in the control and Ad-NC groups, separately, as validated in Transwell assay (Fig. 3B,C, $p < 0.01$), indicating that Ad-SIRT6 infection inhibits keloid fibroblast migration and invasion.

Effect of SIRT6 Overexpression on Collagen Synthesis in Keloid Fibroblasts

Subsequently, the effect of Ad-SIRT6 infection on collagen synthesis in keloid fibroblasts was assessed. Compared to the control and Ad-NC groups, the Ad-SIRT6 group exhibited significant reduction in mRNA and protein levels of α-SMA, collagen I, collagen III, p-Smad3 and TGF-β1 (Fig. 4A,B, $p < 0.001$). A drop of these key markers suggests that Ad-SIRT6 infection can inhibit collagen synthesis in keloid fibroblasts to a certain extent.

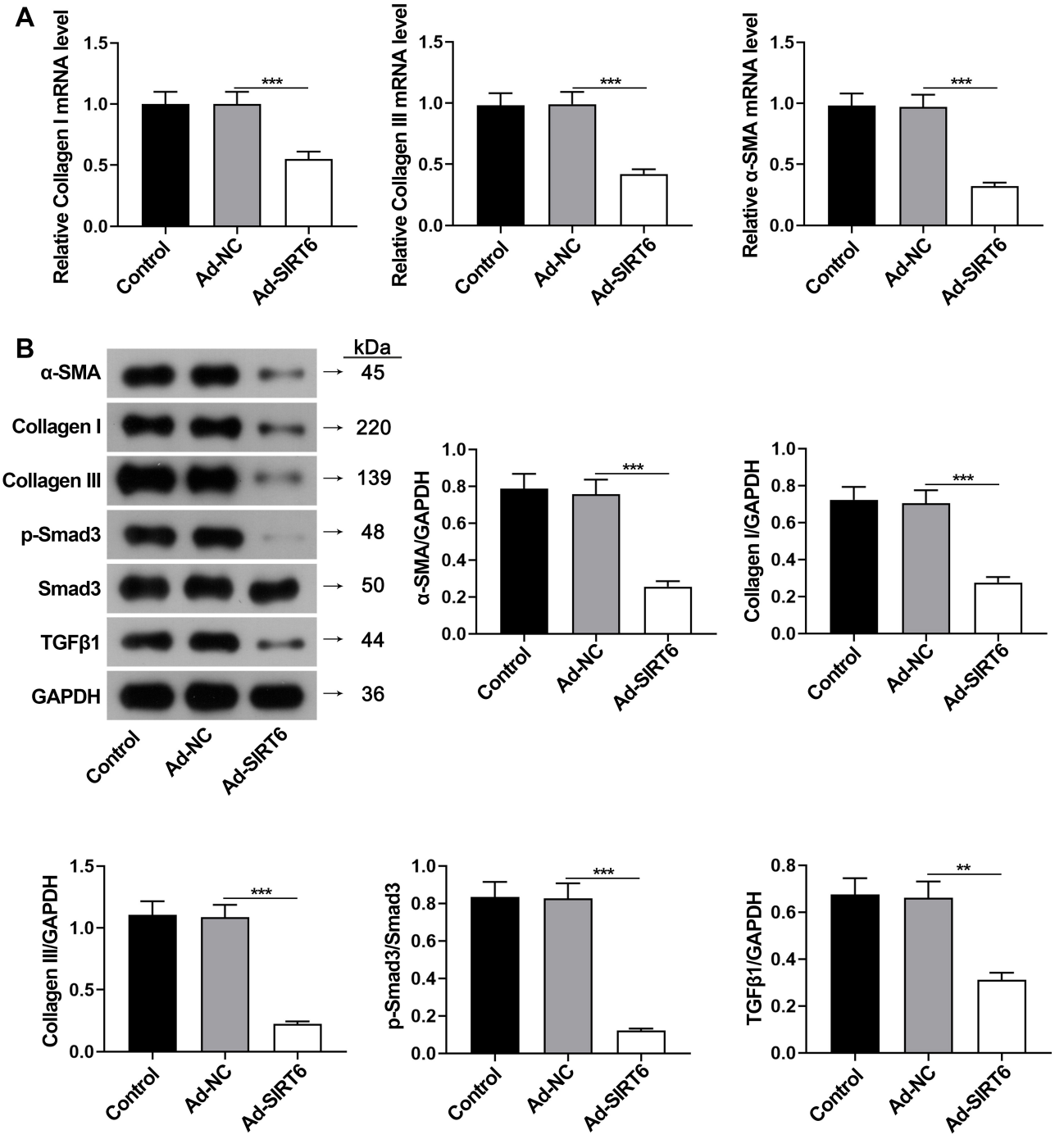

Fig. 4. Effect of SIRT6 overexpression on collagen synthesis in keloid fibroblasts. (A) Estimation of *collagen I*, *collagen III* and *α-SMA* mRNA levels by qRT-PCR. (B) Estimation of α-SMA, collagen I, collagen III, Smad3 and TGF-β1 protein levels through Western blotting. $^{**}p < 0.01$. $^{***}p < 0.001$. n = 3. qRT-PCR, Quantitative reverse transcription polymerase chain reaction; Smad3, phospho SMAD Family Member 3; TGF-β1, transforming growth factor-β 1; *α-SMA*, α-smooth muscle actin.

MAPK/ERK Mediates the Effects of SIRT6 on the Activity of Keloid Fibroblasts

Next, MAPK/ERK-mediated SIRT6 effects on keloid fibroblast activity were assessed. Compared to the control and Ad-NC groups, the Ad-SIRT6 group exhibited significant reduction in protein levels of p-ERK1/2, p-MEK and p-c-Raf (Fig. 5, $p < 0.001$). As shown by the Western blotting results, p-ERK1/2, p-MEK and p-c-Raf protein levels became substantially increased in Ad-SIRT6-infected keloid fibroblasts treated with epidermal growth factor (EGF), an MAPK/ERK pathway agonists (Fig. 6A, $p < 0.05$). EdU assay confirmed that the EdU-positive cell rate was substantially increased in the Ad-SIRT6 group under the treatment of EGF (Fig. 6B, $p < 0.05$). The results showed that the

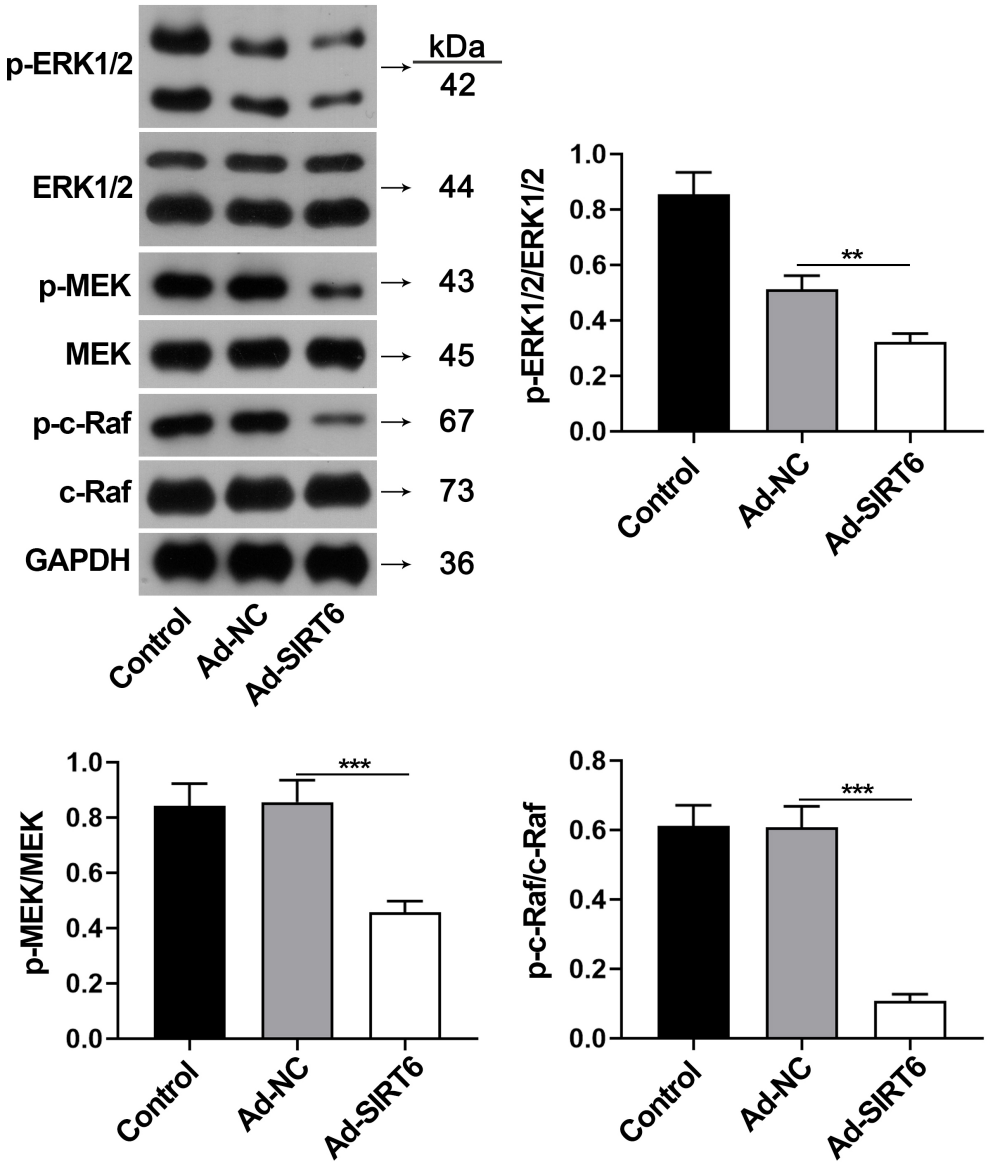

Fig. 5. Effect of SIRT6 overexpression on the expression of MAPK/ERK pathway-related protein, containing p-ERK1/2, ERK1/2, p-MEK, MEK, p-c-Raf, and c-Raf protein levels. $^{**}p < 0.01$. $^{***}p < 0.001$. n = 3. p-ERK1/2, phospho extracellular signal-regulated protein kinase 1/2; p-MEK, phospho MAP kinase-ERK kinase; p-c-Raf, phospho-c-Raf; MAPK/ERK, Mitogen-Activated Protein Kinases (MAPK)/extracellular regulated protein kinases (ERK).

apoptosis rate was inhibited in the Ad-SIRT6+EGF group compared with the control and Ad-SIRT6 groups, as proven via flow cytometry (Fig. 6C, $p < 0.05$), suggesting that SIRT6 is able to hamper keloid fibroblast activity by inhibiting MAPK/ERK pathway.

Discussion

Although keloids resemble tumors in certain aspects, they do not possess the metastatic properties of tumors or exhibit cell heterogeneity, a characteristic of tumors, and an imbalance of apoptosis is closely related to tumorigenesis [11]. Fibroblasts are the main effector cells in keloids, proliferating abnormally and transforming after an injury. Under normal circumstances, a large number of active fibroblasts play an important role in the repair of traumatic injuries, but disruption to this process is an underlying factor of keloid development; therefore, the key to preventing and treating keloid scarring is to inhibit the excessive proliferation of fibroblasts and induce their apoptosis [12,13]. With the widespread application of gene technology in clinical settings, gene therapy holds promise in resolving the pathogenic factor responsible for keloid scarring. In this study, we investigated the role of SIRT6 in the regulation of keloid fibroblast activity, metastasis and collagen synthesis, provide a fundamental insight into the clinical treatment of scars.

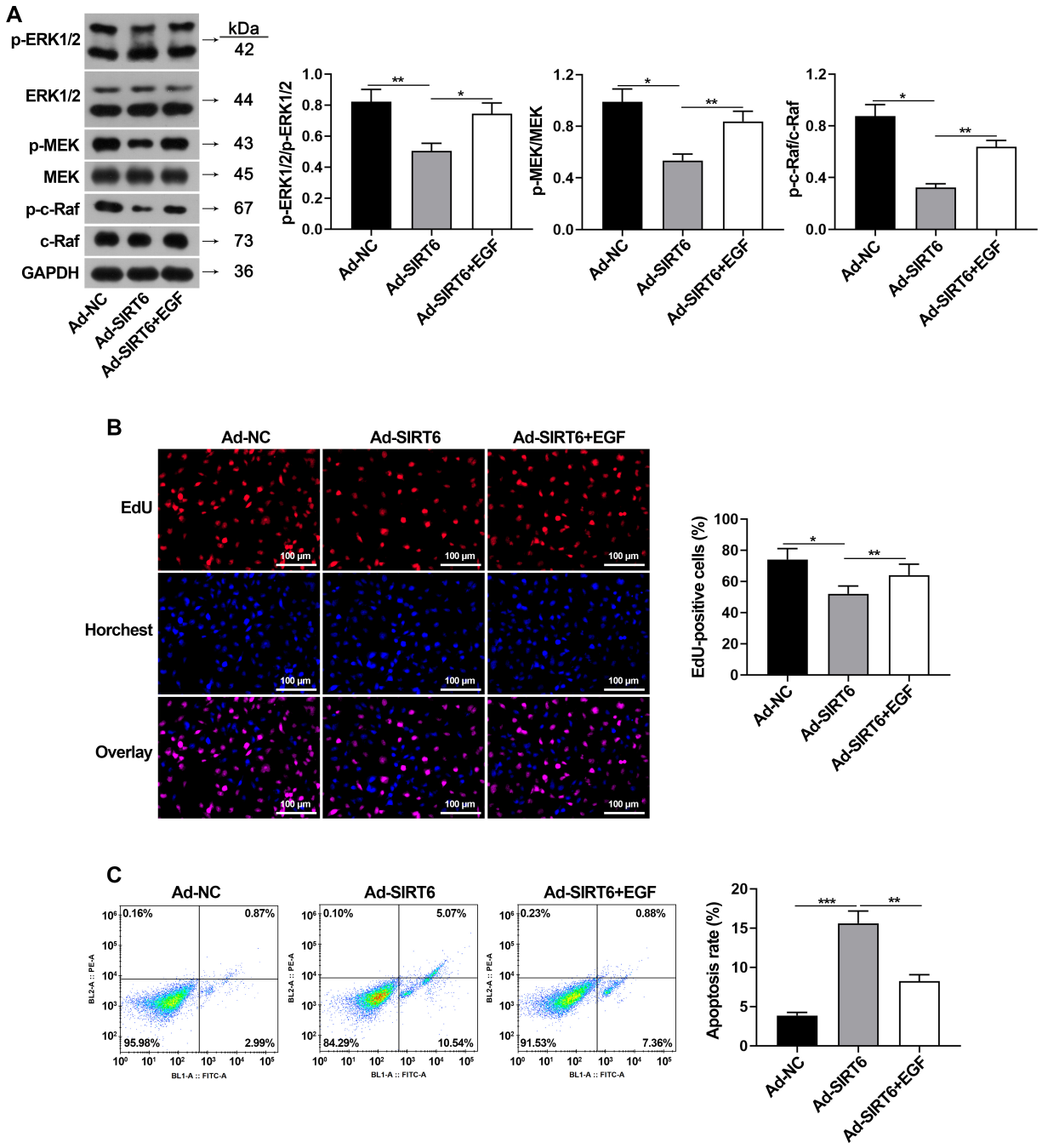

Fig. 6. MAPK/ERK mediates the effect of SIRT6 on keloid fibroblast activity. Keloid fibroblasts were treated with epidermal growth factor (EGF), an MAPK/ERK pathway agonists. (A) Protein level detection of p-ERK1/2, ERK1/2, p-MEK, MEK, p-c-Raf, and c-Raf by means of Western blotting. (B) Cellular activity of keloid fibroblasts visualized by EdU assay. (C) Flow cytometric detection of apoptosis. *$p < 0.05$, **$p < 0.01$, ***$p < 0.001$.

SIRT6 is a multifunctional protein that regulates a wide range of biological functions in the cells [14]. SIRT6 has been reported to inhibit the proliferation and invasion of tumor cells, thus exerting an anticancer function [15,16]. Fibroblasts embody the characteristics of tumor cells, and their hyperproliferation, invasion and collagen deposition collectively serve as an important basis for keloid formation and infiltrative growth, justifying keloids as benign skin tumors. In addition, it has been reported that SIRT6 is highly involved in fibrosis and its mechanism is closely related to the regulation of the MAPK/ERK signaling pathway [7]. In the present study, we speculate that SIRT6 may also have a role in regulating keloids. To test this hypothesis, the present study further investigated the regulatory role of SIRT6 on keloid fibroblast proliferation, invasion and collagen synthesis by isolating and culturing fibroblasts

from keloid scars. This study revealed that SIRT6 overexpression in keloid fibroblasts, achieved with adenovirus-mediated gene overexpression technique, could effectively inhibit cell proliferation and invasion and promote apoptosis. These results suggest that SIRT6 has an inhibitory effect on the abnormal activation of keloid fibroblasts. Therefore, SIRT6 is a novel therapeutic target for keloids.

MAPK is a class of serine or threonine signal transduction enzymes that are highly conserved in eukaryotic cells. Extracellular regulated protein kinases (ERK) is a member of the Mitogen-Activated Protein Kinases (MAPK) family. In particular, the MAPK/ERK signaling pathway is activated by the Ras-Raf-MEK-ERK1/2 signaling axis, which plays a role in cell cycle regulation, tissue development and growth factor secretion [17,18]. The MAPK/ERK pathway is also associated with the development of various fibrotic diseases. For example, it has been shown that neferine exerts antioxidant and anti-inflammatory effects on carbon tetrachloride-induced hepatic fibrosis by inhibiting the MAPK pathway [19]. In addition, selegiline alleviates fibrosis in diabetic nephropathy through the MAPK/ERK signaling pathway [20]. In keloids, protein tyrosine phosphatase 1B regulates fibroblast proliferation, motility and extracellular matrix synthesis via the MAPK/ERK signaling pathway in keloids [21]. In addition, one study has shown that SIRT6 has been reported to be highly involved in fibrosis by regulating the MAPK/ERK signaling pathway [7]. In the current study, we found that SIRT6 was able to inhibit keloid fibroblast proliferation, promote their apoptosis, and inhibit the MAPK/ERK pathway. Therefore, blocking the activation of the MAPK/ERK signaling pathway by upregulating SIRT6 expression, thereby inhibiting the excessive proliferation, invasion and collagen deposition of keloid fibroblasts, stands as a novel strategy for the treatment of keloid scars.

However, several limitations of this study should be acknowledged. This study set out to mainly examine the effect of SIRT6 overexpression on keloid fibroblasts but SIRT6 knockdown assay was not performed for validation purposes. Therefore, follow-up studies should encompass SIRT6 knockdown and functional experiments to confirm the important role of SIRT6 in keloid formation. Future studies could explore the impact of prolonged SIRT6 modulation and utilize animal models to assess the potential for clinical translation. Moreover, whether SIRT6 inhibits the activity of keloid fibroblasts by inhibiting the MAPK/ERK pathway warrants more in-depth experimental verification. Further discussion is needed on how SIRT6 affects specific aspects of the MAPK/ERK pathway, such as whether it directly interacts with the pathway-related proteins, indirectly influences pathway activity through the regulation of other signaling molecules, or affects gene expression via epigenetic modifications.

Conclusion

In summary, this study has demonstrated that the overexpression of SIRT6 significantly inhibits the proliferation, invasion, and collagen synthesis in keloid fibroblasts, while concurrently promoting their apoptosis. These effects are likely mediated through the downregulation of the MAPK/ERK signaling pathway's activity. Importantly, this research unveils novel molecular mechanisms that underlie keloid formation and offers valuable insights into the development of innovative therapeutic strategies targeting SIRT6 for the treatment of keloids.

Availability of Data and Materials

The datasets used and/or analyzed during the current study are available from the corresponding author upon reasonable request.

Author Contributions

TZ designed the research study and wrote the first draft. YJC and CW performed the research. ZYH provided help and advice on the qRT-PCR and Western blotting experiments. ZMT and YM analyzed the data. All authors contributed significantly to editorial changes of important content. All authors read and approved the final manuscript. All authors have participated sufficiently in the work and agreed to be accountable for all aspects of the work.

Ethics Approval and Consent to Participate

This study adheres to the ethical principles of the Helsinki Declaration and was approved by the Chengdu Second People's Hospital ethics committee (No. 2023927723). These patients provided their medical history, as well as informed consent to join this research.

Acknowledgment

Not applicable.

Funding

This research received no external funding.

Conflict of Interest

The authors declare no conflict of interest.

References

[1] Naik PP. Novel targets and therapies for keloid. Clinical and Experimental Dermatology. 2022; 47: 507–515.

[2] Yin Q, Wolkerstorfer A, Niessen FB, Gibbs S, Louter JMI, van Zuijlen PPM, *et al*. Current Practice in Keloid Treatment: a Sur-

vey of Dutch Dermatologists and Plastic Surgeons. Dermatologic Surgery. 2023; 49: 844–850.

[3] Ogawa R, Dohi T, Tosa M, Aoki M, Akaishi S. The Latest Strategy for Keloid and Hypertrophic Scar Prevention and Treatment: The Nippon Medical School (NMS) Protocol. Journal of Nippon Medical School. 2021; 88: 2–9.

[4] Wu D, Liu X, Jin Z. Adipose-derived mesenchymal stem cells-sourced exosomal microRNA-7846-3p suppresses proliferation and pro-angiogenic role of keloid fibroblasts by suppressing neuropilin 2. Journal of Cosmetic Dermatology. 2023; 22: 2333–2342.

[5] Zang C, Liu Y, Chen H. The Sphingolipids Metabolism Mechanism and Associated Molecular Biomarker Investigation in Keloid. Combinatorial Chemistry & High Throughput Screening. 2023; 26: 2003–2012.

[6] Guo Z, Li P, Ge J, Li H. SIRT6 in Aging, Metabolism, Inflammation and Cardiovascular Diseases. Aging and Disease. 2022; 13: 1787–1822.

[7] Chien LH, Deng JS, Jiang WP, Chou YN, Lin JG, Huang GJ. Evaluation of lung protection of Sanghuangporus sanghuang through TLR4/NF-κB/MAPK, keap1/Nrf2/HO-1, CaMKK/AMPK/Sirt1, and TGF-β/SMAD3 signaling pathways mediating apoptosis and autophagy. Biomedicine & Pharmacotherapy. 2023; 165: 115080.

[8] Maity S, Muhamed J, Sarikhani M, Kumar S, Ahamed F, Spurthi KM, *et al*. Sirtuin 6 deficiency transcriptionally up-regulates TGF-β signaling and induces fibrosis in mice. The Journal of Biological Chemistry. 2020; 295: 415–434.

[9] Liu X, Jiang D, Huang W, Teng P, Zhang H, Wei C, *et al*. Sirtuin 6 attenuates angiotensin II-induced vascular adventitial aging in rat aortae by suppressing the NF-κB pathway. Hypertension Research: Official Journal of the Japanese Society of Hypertension. 2021; 44: 770–780.

[10] Fan X, Chen J, Shi D, Jia J, He J, Li L, *et al*. The role and mechanisms of action of SIRT6 in the suppression of postoperative epidural scar formation. International Journal of Molecular Medicine. 2016; 37: 1337–1344.

[11] Hawash AA, Ingrasci G, Nouri K, Yosipovitch G. Pruritus in Keloid Scars: Mechanisms and Treatments. Acta Dermato-venereologica. 2021; 101: adv00582.

[12] Lee SY, Lee AR, Choi JW, Lee CR, Cho KH, Lee JH, *et al*. IL-17 Induces Autophagy Dysfunction to Promote Inflammatory Cell Death and Fibrosis in Keloid Fibroblasts *via* the STAT3 and HIF-1α Dependent Signaling Pathways. Frontiers in Immunology. 2022; 13: 888719.

[13] Chao H, Zheng L, Hsu P, He J, Wu R, Xu S, *et al*. IL-13RA2 downregulation in fibroblasts promotes keloid fibrosis via JAK/STAT6 activation. JCI Insight. 2023; 8: e157091.

[14] Liu G, Chen H, Liu H, Zhang W, Zhou J. Emerging roles of SIRT6 in human diseases and its modulators. Medicinal Research Reviews. 2021; 41: 1089–1137.

[15] Yang Z, Huang R, Wang Y, Guan Q, Li D, Wu Y, *et al*. SIRT6 drives sensitivity to ferroptosis in anaplastic thyroid cancer through NCOA4-dependent autophagy. American Journal of Cancer Research. 2023; 13: 464–474.

[16] Han Q, Xie QR, Li F, Cheng Y, Wu T, Zhang Y, *et al*. Targeted inhibition of SIRT6 via engineered exosomes impairs tumorigenesis and metastasis in prostate cancer. Theranostics. 2021; 11: 6526–6541.

[17] Arafa ESA, Refaey MS, Abd El-Ghafar OAM, Hassanein EHM, Sayed AM. The promising therapeutic potentials of ginsenosides mediated through p38 MAPK signaling inhibition. Heliyon. 2021; 7: e08354.

[18] Zhao Y, Gui W, Niu F, Chong S. The MAPK Signaling Pathways as a Novel Way in Regulation and Treatment of Parasitic Diseases. Diseases (Basel, Switzerland). 2019; 7: 9.

[19] Wang Y, Wang S, Wang R, Li S, Yuan Y. Neferine Exerts Antioxidant and Anti-Inflammatory Effects on Carbon Tetrachloride-Induced Liver Fibrosis by Inhibiting the MAPK and NF-κB/IκBα Pathways. Evidence-based Complementary and Alternative Medicine: ECAM. 2021; 2021: 4136019.

[20] Cheng S, Li L, Song C, Jin H, Ma S, Kang P. Sitagliptin relieves diabetic nephropathy fibrosis via the MAPK/ERK signaling pathway. Minerva Endocrinologica. 2020; 45: 273–275.

[21] Qian L, Wang Q, Wei C, Wang L, Yang Y, Deng X, *et al*. Protein tyrosine phosphatase 1B regulates fibroblasts proliferation, motility and extracellular matrix synthesis via the MAPK/ERK signalling pathway in keloid. Experimental Dermatology. 2022; 31: 202–213.